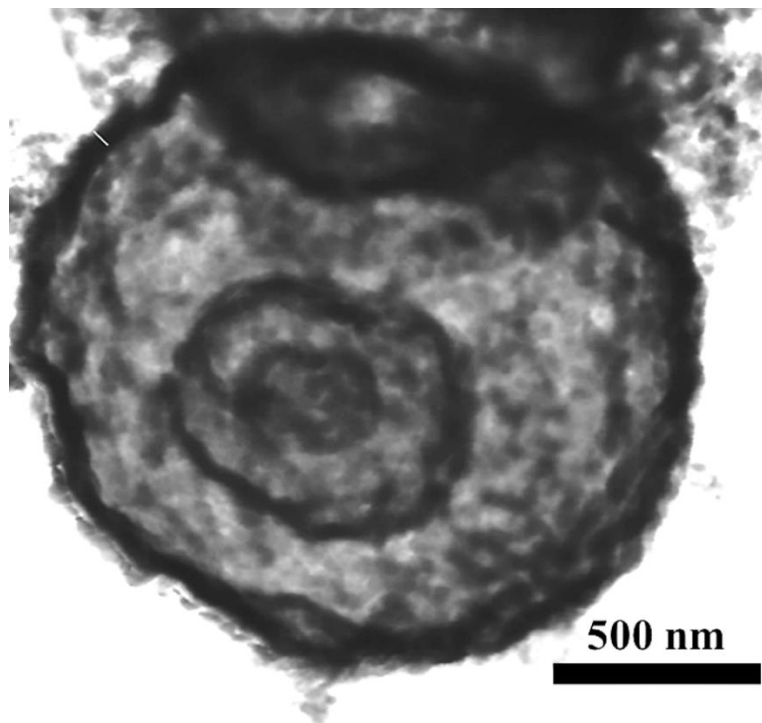
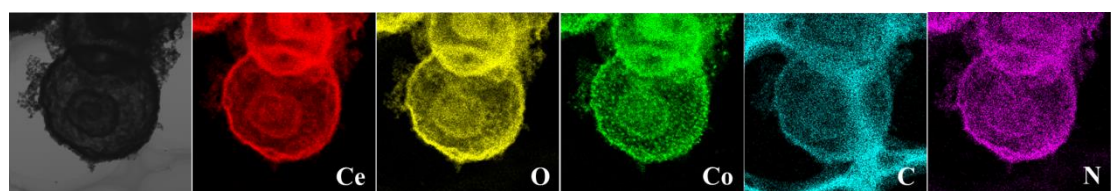


**-Electronic Supplementary Information-**



**Figure S1.** Enlarge TEM images of CeO<sub>2</sub>/Co@NCH.



**Figure S2.** The element mapping of Ce, O, Co, C, N in CeO<sub>2</sub>/Co@NCH.

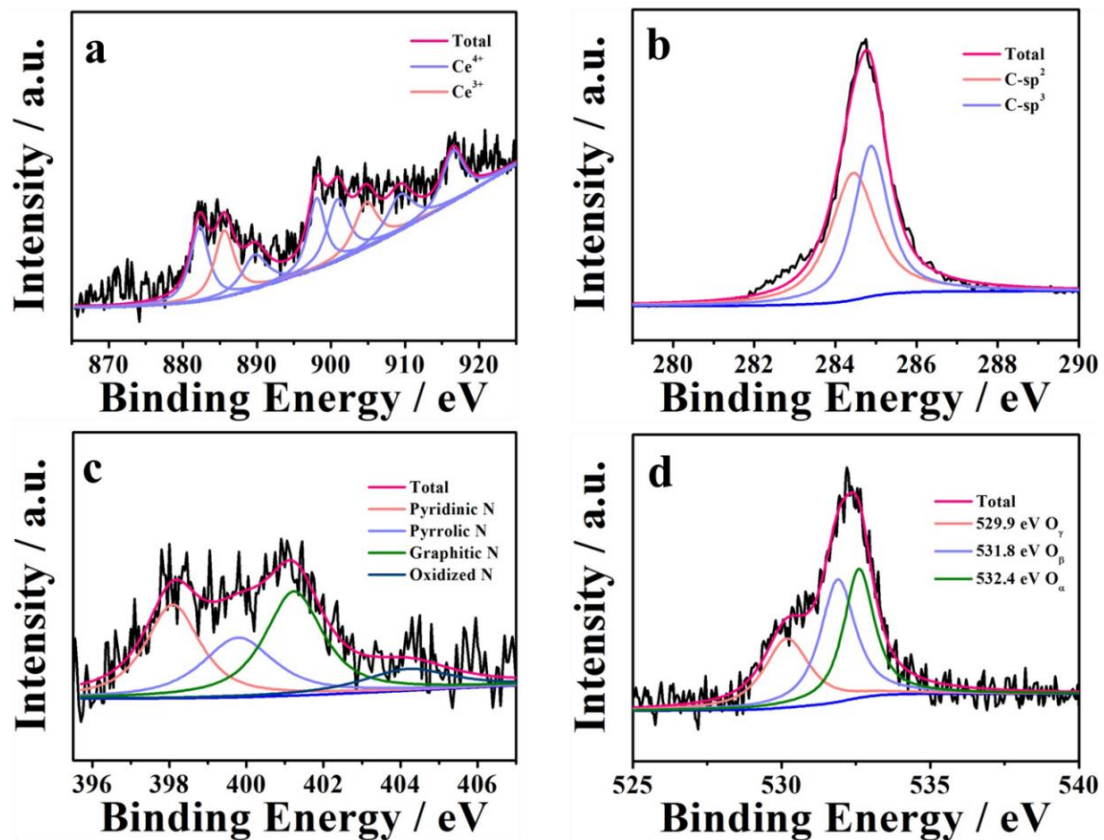


**Figure S3.** XPS high-resolution Ce 3d (a), C 1s (b), N 1s (c) and O 1s (d) spectra of  $\text{CeO}_2@\text{NCH}$ .

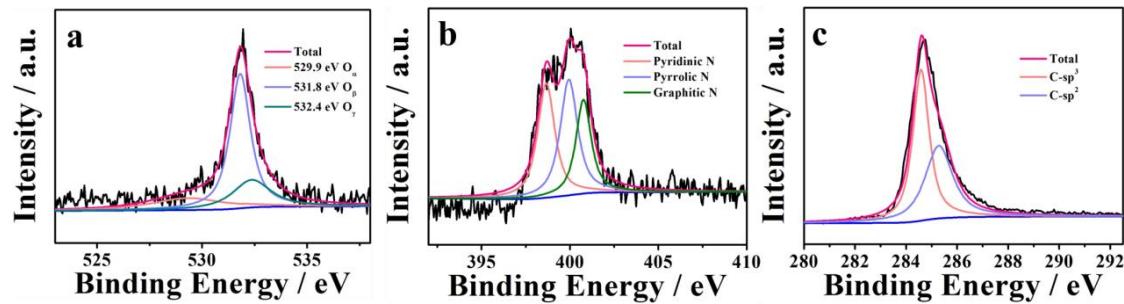


**Figure S4.** XPS high-resolution O 1s (a), N 1s (b) and C 1s (c) spectra of NCH.

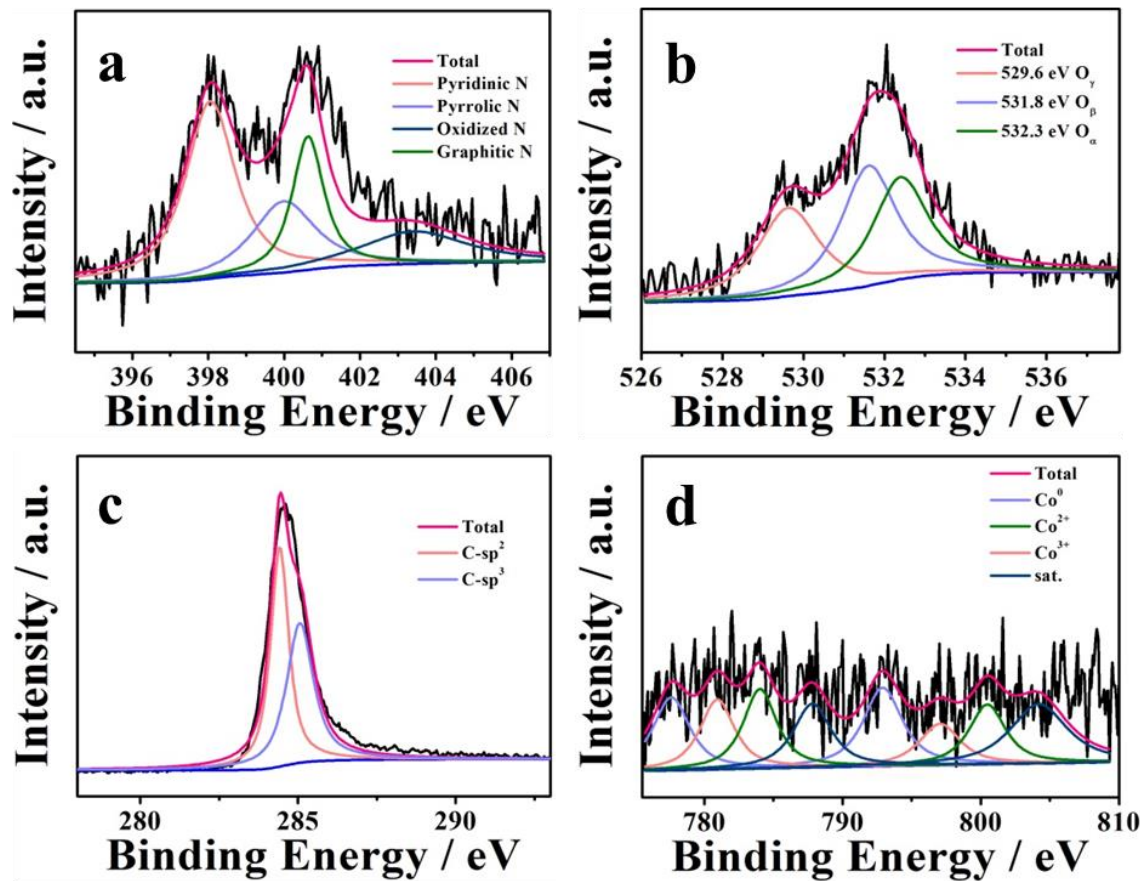


**Figure S5.** XPS high-resolution N 1s (a), O 1s (b), C 1s (c) and Co (d) spectra of Co@NCH.

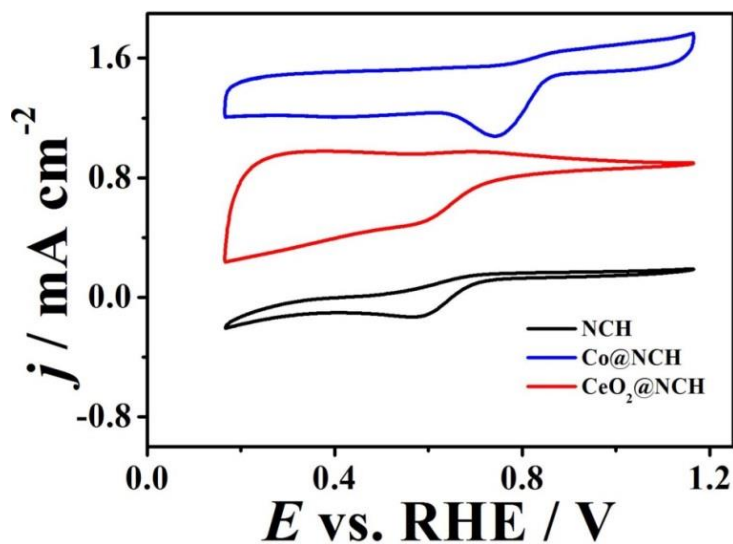


**Figure S6.** CV curves of NCH, Co@NCH and CeO<sub>2</sub>@NCH recorded in O<sub>2</sub> saturated 0.1 M KOH.

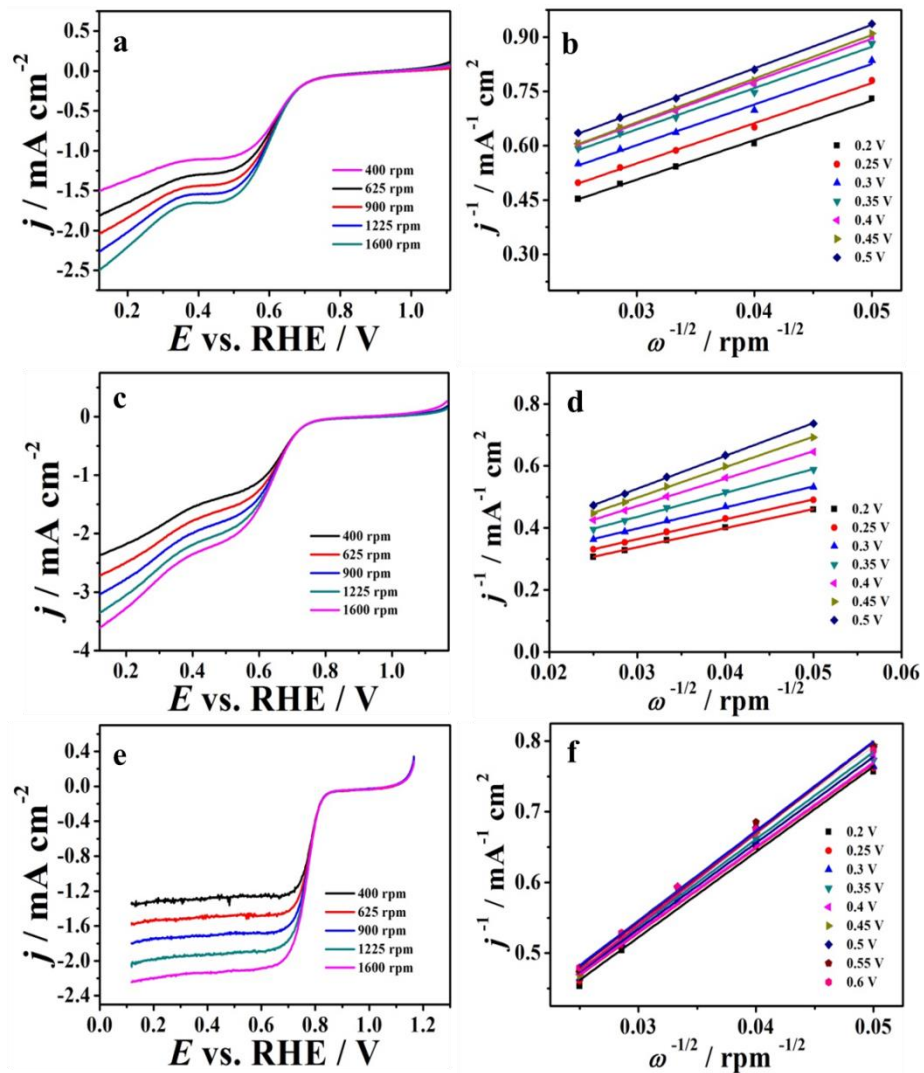


**Figure S7.** LSV curves of NCH, CeO<sub>2</sub>@NCH and Co@NCH measured at different rotating rates and corresponding K-L plots at various potential range.

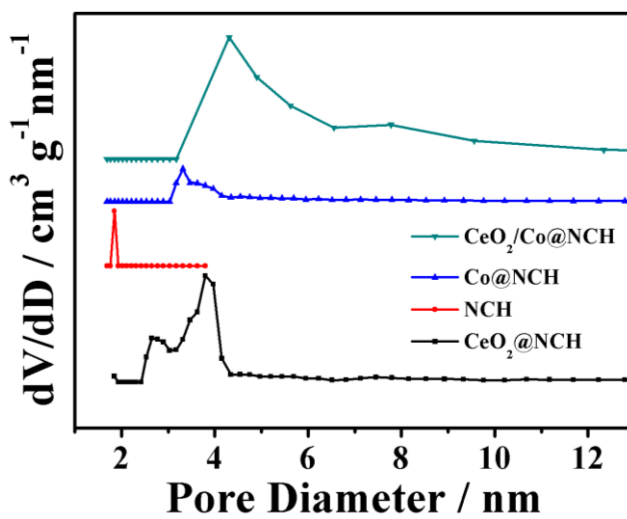


**Figure S8.** The pore size distribution curves of NCH, Co@NCH, CeO<sub>2</sub>@NCH and CeO<sub>2</sub>/Co@NCH.

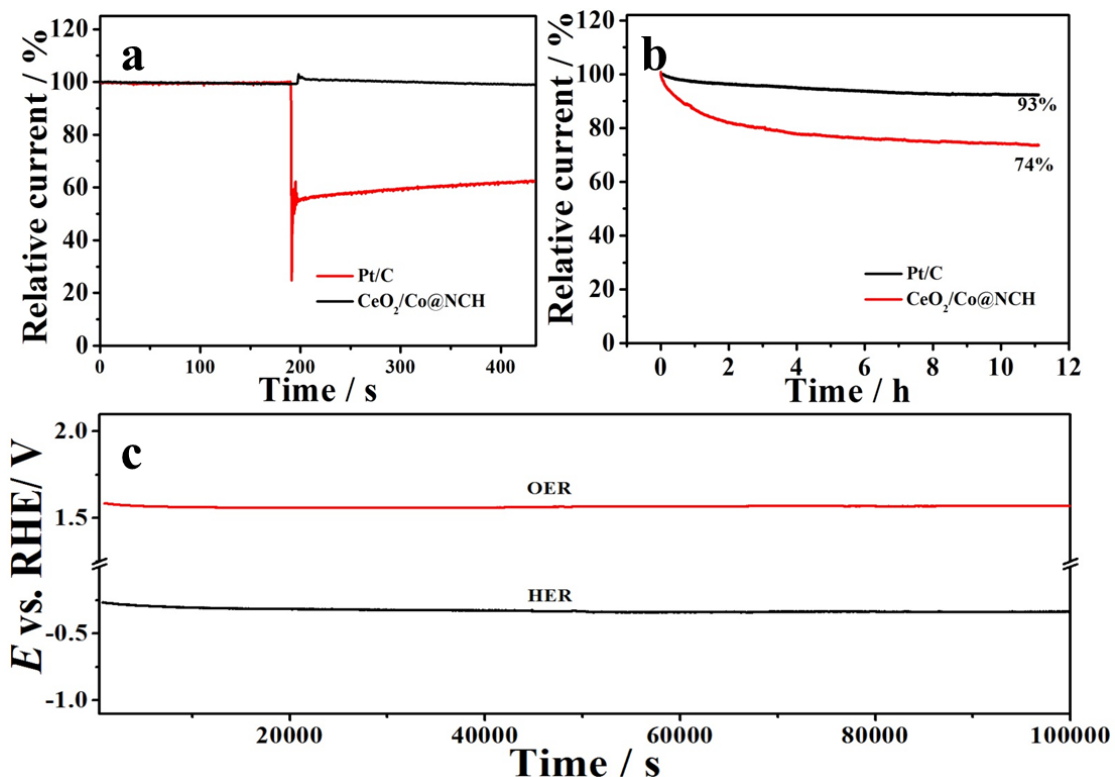


**Figure S9.** (a) methanol tolerance measurement of CeO<sub>2</sub>/Co@NCH and Pt/C samples upon introducing 3M methanol after about 200 s at 0.6 V vs. RHE. (b) i-t chronoamperometric stability measurement of CeO<sub>2</sub>/Co@NCH and Pt/C samples at 0.565 V vs. RHE. (c) The OER and HER stability of CeO<sub>2</sub>/Co@NCH under a constant current density of 10 mA cm<sup>-2</sup> for 100000 s.

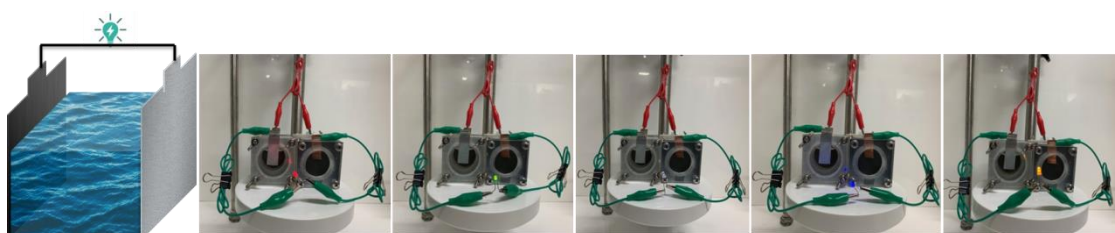


**Figure S10.** (a) Schematic illustration of the rechargeable zinc-air battery. (b) Photograph showing a series of LED powered by two liquid zinc-air batteries with the CeO<sub>2</sub>/Co@NCH cathode connected in series.

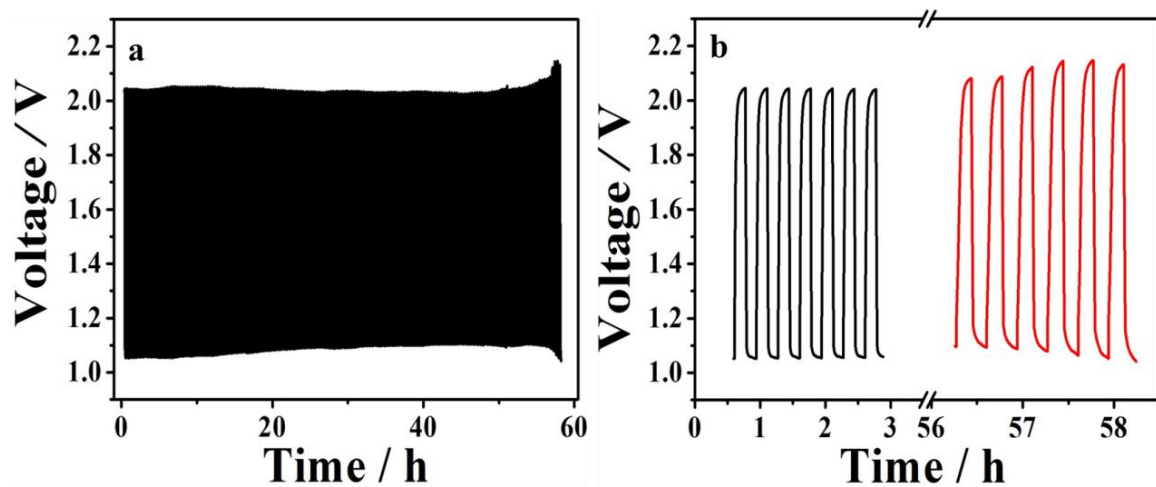


**Figure S11.** Galvanostatic discharge-charge cycling curves at  $5 \text{ mA cm}^{-2}$  of recharged Zn-air batteries with the Pt/C catalyst on carbon paper.

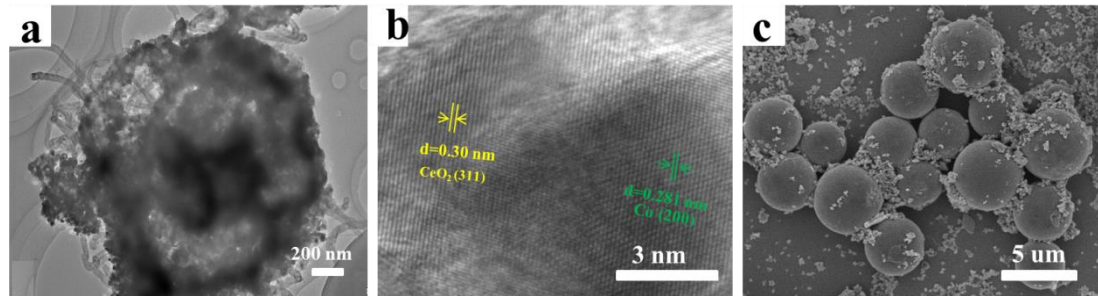


**Figure S12.** TEM (a) HRTEM (b) and SEM (c) images for  $\text{CeO}_2/\text{Co}@\text{NCH}$  after 40000 s chronoamperometric test.

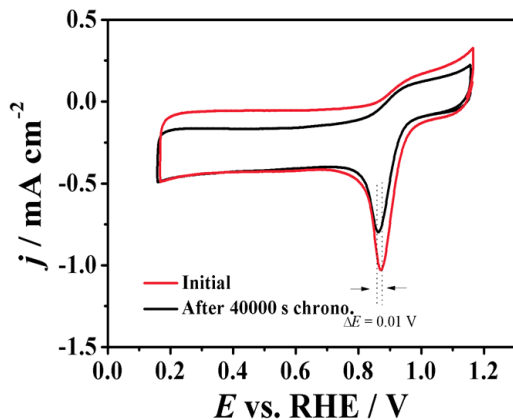


**Figure S13.** CV curves of  $\text{CeO}_2/\text{Co}@\text{NCH}$  in  $\text{O}_2$  saturated 0.1 M KOH solution

before and after 40000 s chronoamperometric test.

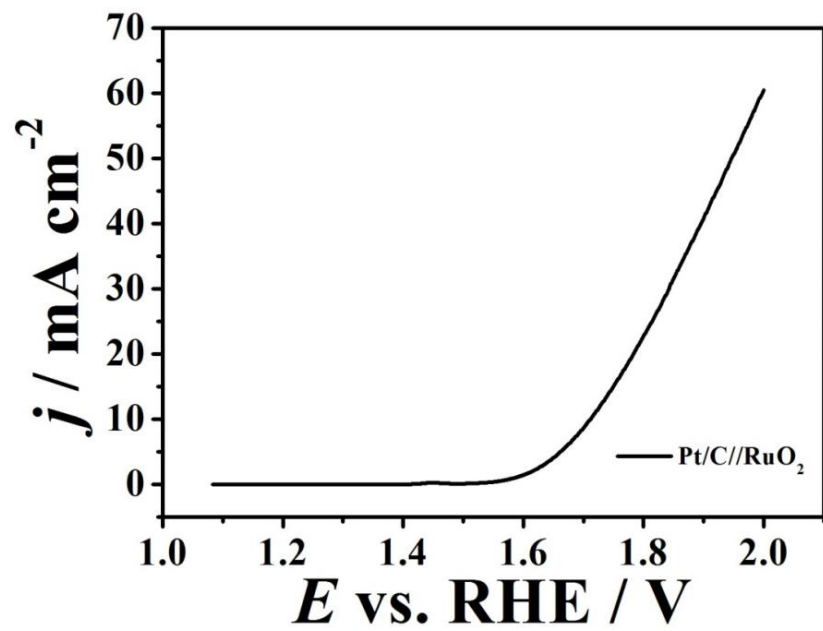


**Figure S14.** Polarization curves of Pt/C||RuO<sub>2</sub> in N<sub>2</sub>-saturated 1M KOH.

**Table S1** Comparison of ORR/OER performances of some reported CeO<sub>2</sub>-based electrocatalysts.

Electrocatalysts	$E_{\text{onset}}$ [V]	$E_{1/2}$ [V]	Medium	$\eta_{\text{OER}} [\text{mV}] @$ $j [\text{mA} \cdot \text{cm}^{-2}]$	$\eta_{\text{HER}} [\text{mV}] @$ $j [\text{mA} \cdot \text{cm}^{-2}]$	Medium	Refs.
CeO <sub>2</sub> /Co(OH) <sub>2</sub> HCs				410@10	317@10	1M KOH	[1]
MoS <sub>2</sub> -G-Ni					>600@10	0.1M KOH	[2]
Ni-Zn/CeO <sub>2</sub>					410@2.74	1M KOH	[3]
g-C <sub>3</sub> N <sub>4</sub> /CeO <sub>2</sub> /Fe <sub>3</sub> O <sub>4</sub>				400@10	310@10	1M KOH	[4]
3D-rGO-CeO <sub>2</sub>					341@10	1 M KOH	[5]
Co <sub>3</sub> O <sub>4</sub> @Z67-NT@CeO <sub>2</sub>	~0.95	0.88	0.1 M	350@10		0.1M KOH	[6]
Ni <sub>2</sub> P-CeO <sub>2</sub> /TM					84@20	1 M KOH	[7]
Fe <sub>x</sub> Ni <sub>y</sub> /CeO <sub>2</sub> /NC				240@10	240@10	1 M KOH	[8]
Co-CeO <sub>2</sub> /N-CNR	~0.90	0.82		410@10		0.1M KOH	[9]
Co@NPC-900	0.88	0.76		380@10		0.1M KOH	[10]
Ni/CeO <sub>2</sub> /CNTs					~220@10	1 M KOH	[11]
CoCe-600N <sub>2</sub>	~0.97	~0.86	0.1 M	274@10		0.1M KOH	[12]
CeO <sub>2</sub> -Cu <sub>3</sub> P/NF					~91@10	1 M KOH	[13]
Co-W/CeO <sub>2</sub>					166@10	1 M NaOH	[14]
Co-CeO <sub>2</sub> -N-C	0.89	0.82	0.1 M	326@10		1 M KOH	[15]
CeO <sub>2</sub> /rGO	0.946	0.84	0.1 M	500@10		0.1M KOH	[16]
CeO <sub>2</sub> nanowires	0.756	0.666	0.1 M	700@10		0.1M KOH	[17]

## References

- [1] M.-C. Sung, G.-H. Lee and D.-W. Kim, *J. Alloys Compd.*, 2019, **800**, 450-455.
- [2] X. Geng, W. Wu, N. Li, W. Sun, J. Armstrong, *Adv. Funct. Mater.*, 2014, **24**, 6123-6129.
- [3] Z. Zheng, N. Li, C.-Q. Wang, D.-Y. Li, F.-Y. Meng and Y.-M. Zhu, *J. Power Sources*, 2013, **222**, 88-91.
- [4] J. Rashid, N. Parveen, T. u. Haq, A. Iqbal, S. H. Talib, S. U. Awan, N. Hussain and M. Zaheer, *ChemCatChem*, 2018, **10**, 5587-5592.

- [5] M. Liu, Z. Ji, X. Shen, H. Zhou, J. Zhu, X. Xie, C. Song, X. Miao, L. Kong and G. Zhu, *Eur. J. Inorg. Chem.*, 2018, **2018**, 3952-3959.
- [6] X. Li, S. You, J. Du, Y. Dai, H. Chen, Z. Cai, N. Ren and J. Zou, *J. Mater. Chem. A*, 2019, **7**, 25853-25864.
- [7] M. Zhang, Q. Dai, H. Zheng, M. Chen and L. Dai, *Adv. Mater.*, 2018, **30**, 1705431.
- [8] L. Chen, H. Jang, M. G. Kim, Q. Qin, X. Liu and J. Cho, *Inorg. Chem. Front.*, 2020, DOI: 10.1039/c9qi01251f.
- [9] A. Sivanantham, P. Ganesan and S. Shanmugam, *Appl. Catal. B*, 2018, **237**, 1148-1159.
- [10] H.-S. Lu, H. Zhang, R. Liu, X. Zhang, H. Zhao and G. Wang, *Appl. Surf. Sci.*, 2017, **392**, 402-409.
- [11] C. Zhang, W. Zhang, N. E. Drewett, X. Wang, S. J. Yoo, H. Wang, T. Deng, J. G. Kim, H. Chen, K. Huang, S. Feng and W. Zheng, *ChemSusChem*, 2019, **12**, 1000-1010.
- [12] X. He, X. Yi, F. Yin, B. Chen, G. Li and H. Yin, *J. Mater. Chem. A*, 2019, **7**, 6753-6765.
- [13] Z. Wang, H. Du, Z. Liu, H. Wang, A. M. Asiri and X. Sun, *Nanoscale*, 2018, **10**, 2213-2217.
- [14] M. Sheng, W. Weng, Y. Wang, Q. Wu and S. Hou, *J. Alloys Compd.*, 2018, **743**, 682-690.
- [15] Z. Zhang, D. Gao, D. Xue, Y. Liu, P. Liu, J. Zhang and J. Qian, *Nanotechnol.*, 2019, **30**, 395401.
- [16] L. Sun, L. Zhou, C. Yang and Y. Yuan, *Int. J. Hydrogen Energy*, 2017, **42**, 15140-15148.
- [17] Y. Yang, T. Yue, Y. Wang, Z. Yang and X. Jin, *Microchem. J.*, 2019, **148**, 42-50.